Modeling diverse physics of nanoparticle self-assembly in pulsed laser-irradiated metallic films

Mikhail Khenner

Department of Mathematics and Computer Science, Western Kentucky University

Several versions of this talk have been presented at: WKU Physics Colloquium, April 25, 2011; 35th SIAM-SEAS Conference, Charlotte, NC, March 26-27, 2011; University of Kentucky Applied Mathematics Seminar, Nov. 8, 2010; Fall Meeting of the Materials Research Society, Boston, MA, Nov. 30 - Bec. 2, 2009; WKU 29th Annual Mathematics Symposium, Nov. 5, 2009; Applied Mathematics Colloquium, Wright State University, Dayton, OH, Oct. 9, 2009

Outline

- Motivation for modeling, challenges
- Single layer films
  - Model description
  - Lubrication and 2D approximations
    (i) Uniform irradiation: Stability analysis
    (ii) Computations of the nonlinear dynamics of the film
- Bilayer films
  (i) Model equations (2D)
  (ii) Stability analysis, simulations
- Future work

lDewetting ≡ "uncovering" (exposure) of some areas the substrate

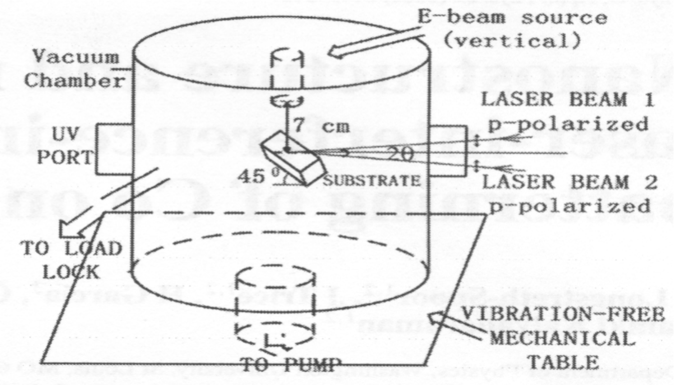

Figure courtesy of R. Kalyanaraman, UTK

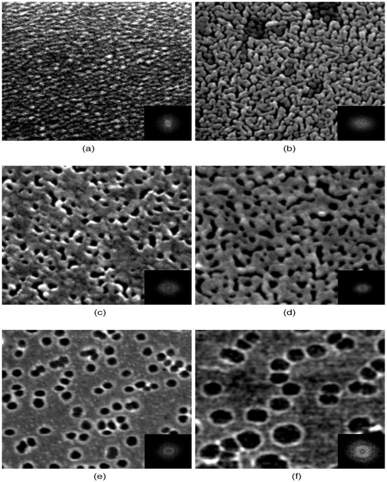

Irradiation by 10 laser pulses. Ag film thickness from (a) to (f): 2, 4.5, 7.4, **9.5**, **11.5**, 20 nm. (Figure courtesy of R. Kalyanaraman, UTK)

Single-layer films, one laser beam: Progression of dewetting towards formation of nanoparticles

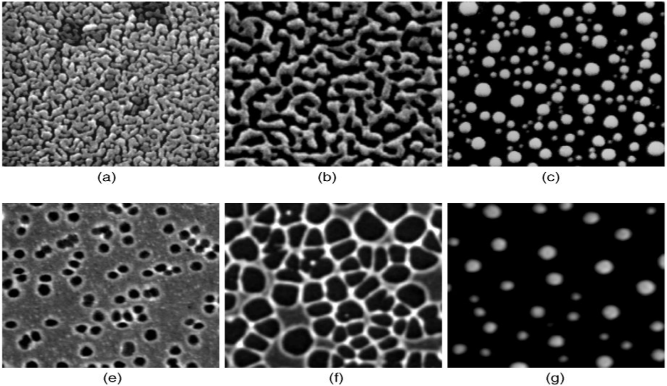

Top row: 4.5 nm thick Ag film. (a)-(c): 10, 100, 10500 laser pulses. Bottom row: 11.5 nm thick Ag film. (e)-(g): 10, 100, 10500 laser pulses. (Figure courtesy of R. Kalyanaraman, UTK)

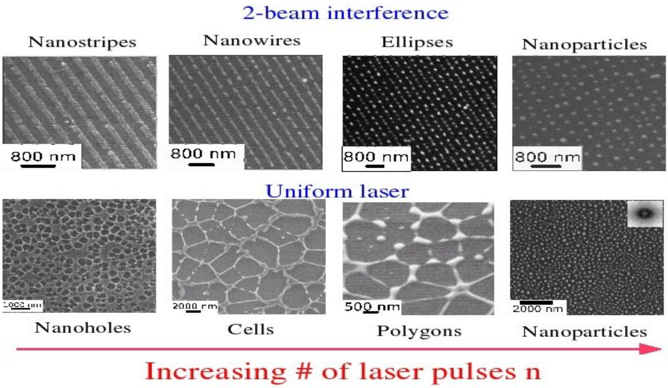

Figure courtesy of R. Kalyanaraman, UTK

Laser interference irradiation

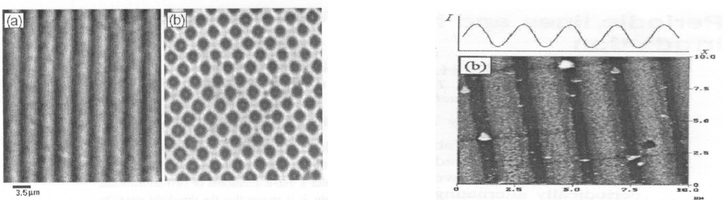

Figure:
Left: Micrographs of 1D and 2D optical interference gratings created on a Au film of 18 nm thickness. (a) "two-beam" and (b) "four-beam" gratings.
Right: AFM image of 8 nm Au film after two-beam interference irradiation. Note that film material accumulates in cold regions. (From Y. Kaganovskii *et al.*, JAP 100, 044317, 2006)

Vision of a multifunctional nanostructured surface platform based on multi-layer films

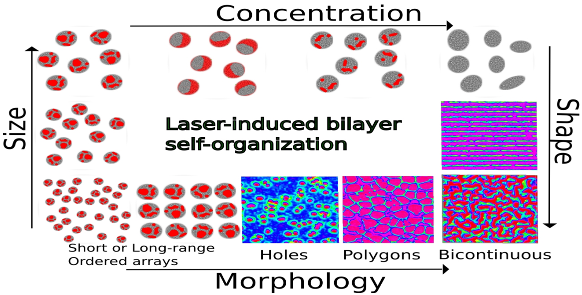

Pulsed laser self-organization of multilayer films made from immiscible materials, like Co and Ag, can be used to synthesize a matrix of discrete micro-regions with varying nanoscale morphology, size, shape, and composition. *Thus a platform with unique multifunctional behavior for sensing and detection can be made.* (Figure courtesy of R. Kalyanaraman, UTK)

Challenges:

- Understand film instabilities resulting in nanopatterning
- Develop a realistic model of heat transfer within the film
- Develop a model of interference control of a pattern formation
- For bilayers, develop models that account for interdiffusion and chemical reactions
- Develop efficient computational methods for 3D simulations (especially for a bilayer system)

Our interest is to model the complete dewetting cycle - from a continuous film to a nanoparticles state

Modeling assumption

Film is liquid at all times, and dewetting is modeled as continuous in time.

In reality, pulse width = 10 ns, pulse frequency = 50 Hz. Nanometer-scale film is:

- Melted "instantaneously" when a pulse hits (energy flux $\sim 10^{11}$ J/sm^2);
- Dewets while the pulse lasts;
- Solidifies "instantaneously" after the pulse is gone, freezing the instantaneous morphology;
- Next pulse quenches in the morphology and the cycle repeats.

Single layer films

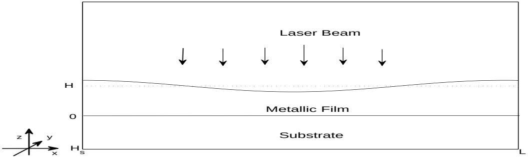

Major physical factors contributing to pattern formation through film dewetting:

- Capillary fluid flow (minimization of the surface area at given fluid volume by the surface tension)
- Unusual, thickness-dependent heat transfer in the film - due to nonlinear optical absorption of light and nonlinear reflectivity
- Thermocapillary (Marangoni) fluid flow arising due to the surface tension dependence on temperature
- Long-range intermolecular (van der Waals) forces between the substrate and film surface molecules

- Molten metal is an incompressible Newtonian liquid.
- Surface tension decreases linearly with increasing temperature

$$\sigma = \sigma_m - \gamma (T - T_m), \quad T > T_m, \quad \gamma > 0$$

- $H/L = \epsilon \ll 1$, also $H_s \sim 10 \div 20H \rightarrow$ **will derive model equations in the lubrication (longwave) approximation**.

  Lubrication approximation is, essentially, a procedure of systematic scalings of governing equations (Navier-Stokes) and expansion of all fields in powers of small parameter ϵ. Lubrication equations are the equations that result in the leading zeroth-order (ϵ^0) of such expansion (Oron, Davis, and Bankoff, *Reviews of Modern Physics* (1997); Craster and Matar, *Reviews of Modern Physics* (2009)).

- Momentum equation (Stokes) and continuity equation

$$\nabla \cdot \mathbf{\Omega} + \rho \mathbf{g} = 0, \quad \nabla \cdot \mathbf{u} = 0 \tag{1}$$

- Energy equation

$$\frac{\kappa}{\rho c_p} \nabla^2 T + Q = 0, \tag{2}$$

where

$$\mathbf{\Omega} = -P\delta_{ij} + \eta \left(\frac{\partial u_i}{\partial x_j} + \frac{\partial u_j}{\partial x_i} \right) : \text{stress tensor}$$

$$Q = \frac{\delta J(1 - R(h))}{2} f(x, y, t) \exp\left(\delta(z - h)\right) \quad \text{(Beer-Lambert law)}$$

$$(0 \leq R(h) < 1 : \text{nonlinear reflectivity})$$

Remark 1: Nonuniformity in the plane of the film enters through $f(x, y, t)$.

At the free surface:

(i) The normal and shear stress balances;

$$\mathbf{n}\cdot\mathbf{\Omega}\cdot\mathbf{n} = -\sigma\nabla\cdot\mathbf{n} + \Pi, \quad \mathbf{t}\cdot\mathbf{\Omega}\cdot\mathbf{n} = \mathbf{t}\cdot\nabla\sigma$$

where $\Pi = (A/6\pi)h^{-3}$ is the **disjoining pressure** due to long-range intermolecular attraction

(ii) The kinematic condition:
$u_3 = h_t + u_1 h_x + u_2 h_y$ $\leftarrow$ **this condition is used to derive the evolution PDE for h after u_1 an u_2 have been averaged in the z-direction**

(iii) Newton's law of cooling:
$\kappa T_z = -\alpha_h (T - T_a)$

At the film-substrate interface:

- No-slip: $u_1 = u_2 = 0$
- No-penetration: $u_3 = 0$
- Continuity of temperature and thermal flux:

$$T = \theta, \quad \kappa T_z = \kappa_s \theta_z, \tag{3}$$

where θ is the temperature field in the substrate, which is obtained by solving the heat conduction equation

$$\frac{\kappa_s}{\rho_s c_{ps}} \nabla^2 \theta + Q = 0 \tag{4}$$

given $R(h) = 0$ in the optically transparent substrate (such as SiO_2) and the boundary condition $z = -H_s : \quad \theta = T_s$

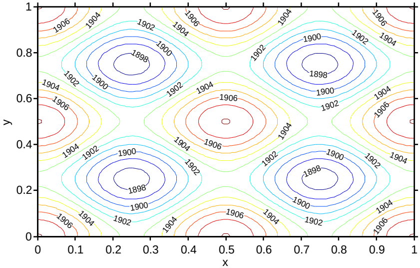

Figure: Surface temperature when four-beam interference is active, modeled by $f \equiv f(x, y) = 1 + 0.1\cos(4\pi(x - 1/2))\cos(4\pi(y - 1/2))$

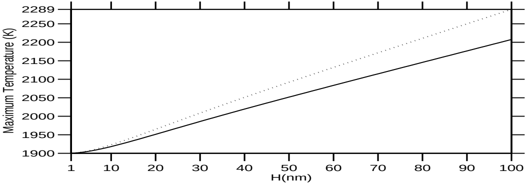

Figure: Plot of the maximum film temperature vs. film height. Dot curve: $R(h) = 0$; solid curve: $R(h) = r_0\,(1 - \exp(-a_r h))$.

$$
\begin{aligned}
h_t &= \frac{\partial}{\partial x}\Big[-(C/3)h^3 h_{xxx} + (G/3)h^3 h_x - A h^{-1} h_x \\
&\quad + M\beta(T_a - T_s)h^2 h_x \\
&\quad + \big\{-M F_h(1-R(h)) + M R'(h) F - M\beta(h+\Psi)R'(h)F \\
&\quad + M\beta(1-R(h))\left(F + (h+\Psi)F_h\right)\big\} f(x,y,t) h^2 h_x\Big]
\end{aligned}
$$

Lines 3 and 4: unconventional terms that emerge due to laser heating

C: capillary numer, G: gravity number, β: Biot number, M: Marangoni number, T_a: ambient temperature, T_s: substrate temperature, A: Hamaker constant, $D = \delta H$: optical thickness, $\Psi = H_s/H\Gamma$, where $\Gamma = \kappa/\kappa_s$

$$
\begin{aligned}
R(h) &= r_0\left(1 - \exp\left(-a_r h\right)\right), \\
F(h, D, \Psi) &= \left(-\Psi + \exp\left(-Dh\right)(\Psi - 1/D) - h + 1/D\right)/2
\end{aligned}
$$

Take $f = 1$**,** $h = 1 + \xi(x,t) = 1 + e^{\omega t}\cos kx$ **and linearize in** ξ**:**

$$\begin{aligned} \omega(k) &= -\frac{G}{3}k^2 - \frac{\epsilon^3}{3C}k^4 + Ak^2 - M\beta(T_a - T_s)k^2 \\ &\quad + MR'F(-1 + \beta(1+\Psi))k^2 \\ &\quad + M(1-R)\left(F_h - \beta\left(F + (1+\Psi)F_h\right)\right)k^2. \end{aligned} \tag{5}$$

$h = 1$: Dimensionless film height at $t = 0$
$\xi(x,t)$: Small perturbation
ω : Growth rate of the perturbation
k : Wavenumber of the perturbation (wavelength $= 2\pi/k$)
R, R', F, F_h are evaluated at $h = 1$

Linear stability analysis (II)

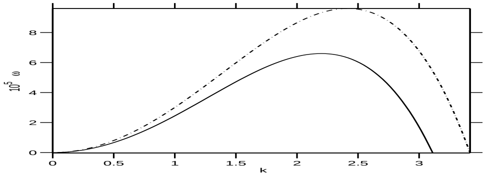

Figure: Variation of ω with k: Dash-dot curve: heat source is zero; solid curve: heat source is non-zero.

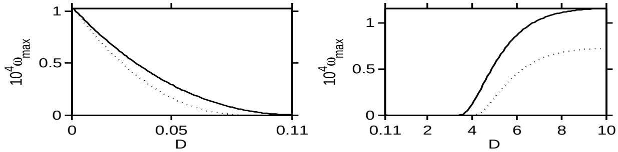

Figure: Variation of ω_{max} with D. Dot curve: $R(h) = 0$; solid curve: $R(h) \neq 0$.

The uniformly heated film is completely stable against small perturbations in some interval of the optical thickness parameter

Single laser beam (no interference, i.e. $f = 1$):

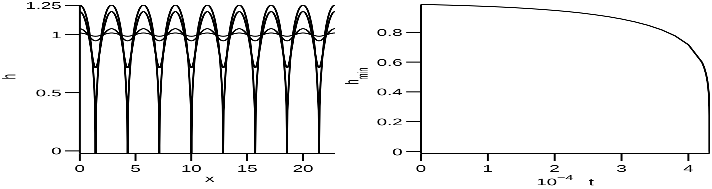

Figure: Profile of the film height (left), and the evolution of the minimum point on the film surface (right). Note the formation of a nanowire array. Spacing equals $2\pi/k_{max} \equiv$ wavelength of the fastest growing perturbation ($\omega = \omega_{max}$).

Rupture time $T_r \approx 0.9$ ms (depends on the amplitude of the initial film height).

Two-beam interference: $f \equiv f(x) = 1 + 0.99\cos(0.157(x - \frac{\pi}{2.2}))$
Note: $2\pi/0.157 = 40$**: the distance between interference fringes**

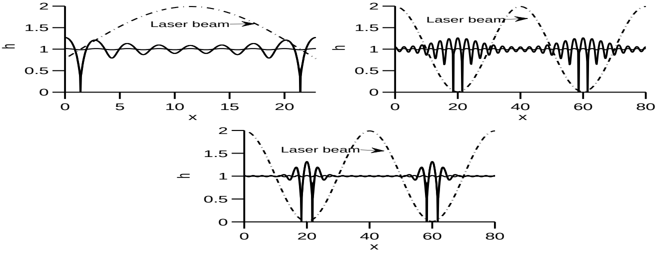

Figure: Top row, left: $H = 10$ nm, 8 wavelengths; Top row, right: $H = 10$ nm, 28 wavelengths; Bottom row: $H = 15$ nm, 28 wavelengths.

The spatial periodicity of nanowires follows the interference imprint.

Bilayer films
(Interference not included yet; 2D analysis)

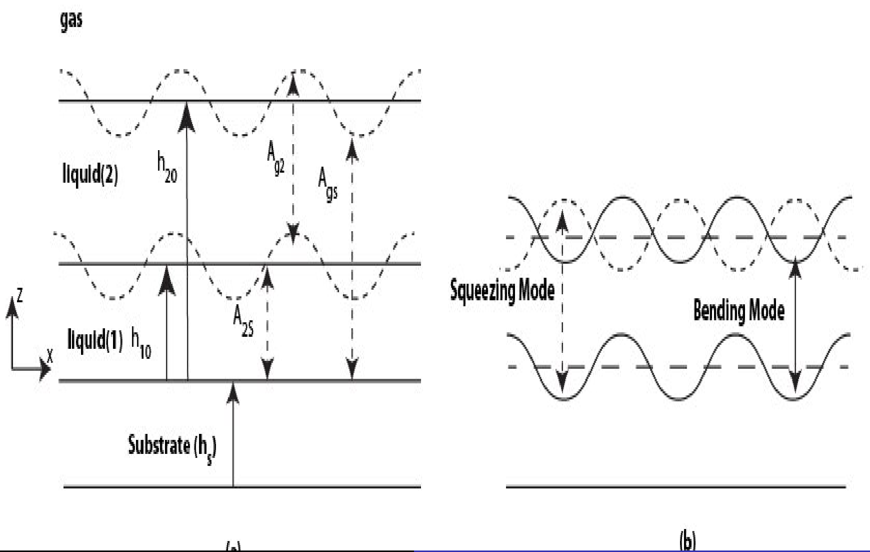
gas
liquid(2)
h_{20}
A_{g2}
A_{gs}
liquid(1)
h_{10}
A_{2S}
z
x
Substrate (h_s)
Squeezing Mode
Bending Mode
(b)

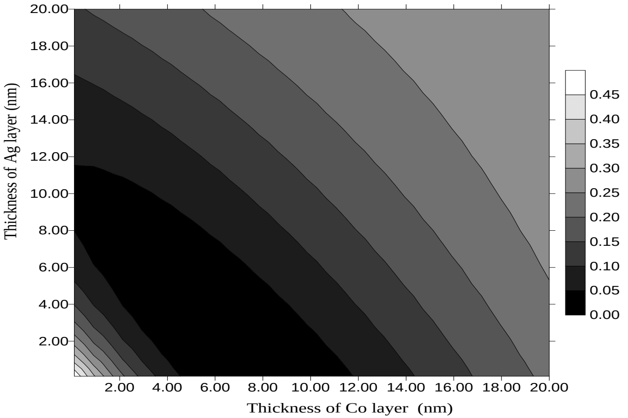

$R = R(h_1, h_2 - h_1)$ is a smooth convex function of its arguments; model adapted from J.S.C. Prentice, "Coherent, partially coherent and incoherent light absorption in thin-film multilayer structures," J. Phys. D: Appl. Phys. **33**, 3139 (2000).

$$
\begin{aligned}
\partial_t h_1 + \partial_x \left[F_{11}\partial_x P_1 + F_{12}\partial_x P_2 + \Phi_{11}\partial_x\sigma_1 + \Phi_{12}\partial_x\sigma_2 \right] &= 0, \\
\partial_t h_2 + \partial_x \left[F_{21}\partial_x P_1 + F_{22}\partial_x P_2 + \Phi_{21}\partial_x\sigma_1 + \Phi_{22}\partial_x\sigma_2 \right] &= 0,
\end{aligned}
$$

$F_{\ell m}(h_1, h_2 - h_1)$ and $\Phi_{\ell m}(h_1, h_2 - h_1)$ are polynomials of a degree at most three, and $\sigma_i = \sigma_i(T_i(h_i(x,t)))$ (next slide)

Pressures:

$$
\begin{aligned}
P_1 &= -\sigma_1\partial_{xx}h_1 - \sigma_2\partial_{xx}h_2 + \Pi_1 + \Pi_2 + \rho_1 g h_1 + \rho_2 g(h_2 - h_1), \\
P_2 &= -\sigma_2\partial_{xx}h_2 + \Pi_2 + \rho_2 g h_2,
\end{aligned}
$$

Disjoining pressures:

$$
\begin{aligned}
\Pi_1(h_1, h_2 - h_1) &= \frac{A_{s2}}{h_1^3} - \frac{A_{g2}}{(h_2 - h_1)^3} + \frac{S_1 \exp\left(-\frac{h_1}{\ell_1}\right)}{l_1} - \frac{S_2 \exp\left(-\frac{(h_2 - h_1)}{\ell_2}\right)}{l_2}, \\
\Pi_2(h_1, h_2 - h_1) &= \frac{A_{g2}}{(h_2 - h_1)^3} + \frac{A_{sg}}{h_2^3} + \frac{S_2 \exp\left(-\frac{(h_2 - h_1)}{\ell_2}\right)}{l_2}.
\end{aligned}
$$

Energy equations:

$$\begin{aligned}\frac{\kappa_{1,2}}{\rho_{1,2} C_{eff}} \partial_{zz} T_{1,2} + \frac{\delta_2}{\rho_{1,2} C_{eff}} J\left(1 - R\right) \exp\left(\delta_{1,2}\left(z - h_2\right)\right) &= 0, \\ \frac{\kappa_s}{\rho_s C_{eff}} \partial_{zz} T_s &= 0.\end{aligned}$$

(Add physical boundary conditions on all three intefaces and solve using CAS)

Surface tensions decrease linearly with increasing temperature:

$$\begin{aligned}\sigma_1 &= \sigma_1^{(m)} - \gamma_1 \left(T_1\left(z = h_1\right) - T_1^{(m)}\right), \quad \gamma_1 > 0,\ T_1\left(z = h_1\right) > T_1^{(m)}, \\ \sigma_2 &= \sigma_2^{(m)} - \gamma_2 \left(T_2\left(z = h_2\right) - T_2^{(m)}\right), \quad \gamma_2 > 0,\ T_2\left(z = h_2\right) > T_2^{(m)},\end{aligned}$$

Co thickness = 5 nm fixed, Ag thickness varies

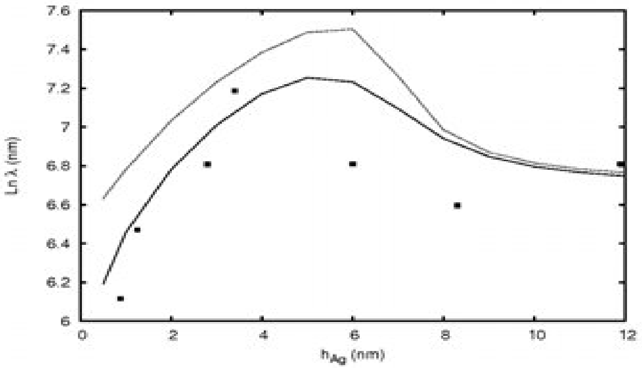

Solid squares: experimental points; Solid line: nonisothermal model; dashed line: isothermal model ($T_i = const.$, $\sigma_i = const.$, thus no thermocapillary (Marangoni) effect)

Co thickness = 5 nm fixed, Ag thickness = 5 nm (left), = 11 nm (right)
Evolves in bending mode

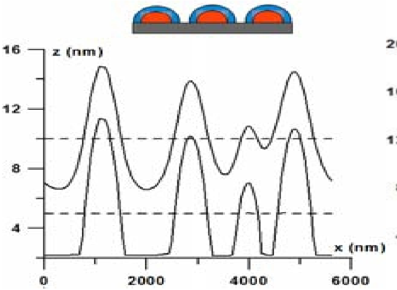

Core-shell wires

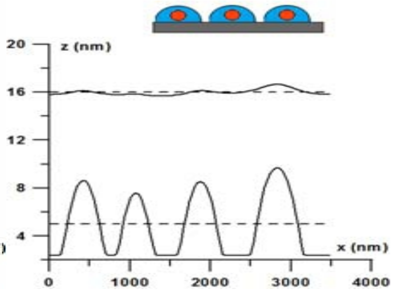

Embedded wires

Outcomes as for AgCo (*core-shell, embedded*), and also *stacked*
Evolves in bending mode

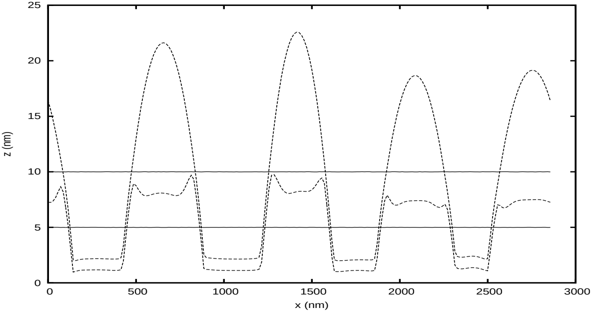

Stacked wires

Tentatively, only the bending mode of evolution results in practically useful outcomes, such as core-shell, embedded, or stacked.

We derived criterium for mode type in the linear regime (small t).

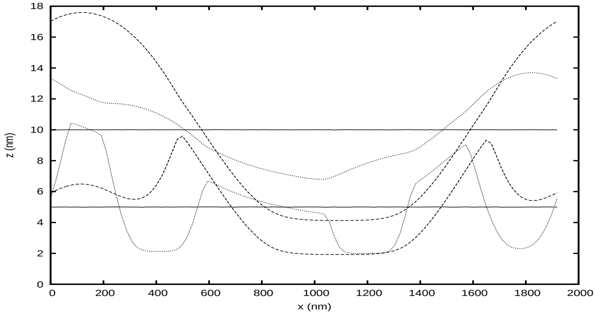

Squeezing mode

Future Work

- Inclusion of interference (bilayer model)
- Inclusion of interdiffusion and chemical reactions (bilayer model)
- Development of the efficient FD code for 3D simulations

Publications:

1. A. Atena and M. Khenner, "Thermocapillary effects in driven dewetting and self-assembly of pulsed laser-irradiated metallic films", Phys. Rev. B 80, 075402 (2009)
2. H. Krishna, R. Sachan, J. Strader, C. Favazza, M. Khenner, and R. Kalyanaraman, "Thickness-dependent spontaneous dewetting morphology of ultrathin Ag films", Nanotechnology 21, (2010) 155601
3. M. Khenner, S. Yadavali, and R. Kalyanaraman, "Formation of organized nanostructures from unstable bilayers of thin metallic liquids" (submitted)